

Evidence for magnetic phase separation in  $\text{La}_{0.86}\text{Sr}_{0.14}\text{Mn}_{1-x}\text{Cu}_x\text{O}_{3+\delta}$  manganites from NMR and magnetic measurements

This article has been downloaded from IOPscience. Please scroll down to see the full text article.

2008 J. Phys.: Condens. Matter 20 095214

(<http://iopscience.iop.org/0953-8984/20/9/095214>)

View [the table of contents for this issue](#), or go to the [journal homepage](#) for more

Download details:

IP Address: 129.252.86.83

The article was downloaded on 29/05/2010 at 10:41

Please note that [terms and conditions apply](#).

# Evidence for magnetic phase separation in $\text{La}_{0.86}\text{Sr}_{0.14}\text{Mn}_{1-x}\text{Cu}_x\text{O}_{3+\delta}$ manganites from NMR and magnetic measurements

Jair C C Freitas<sup>1,4</sup>, Rodolfo A Victor<sup>1</sup>, Marcos T D Orlando<sup>1</sup>,  
Armando Y Takeuchi<sup>1</sup>, Ivan S Oliveira<sup>2</sup> and Tito J Bonagamba<sup>3</sup>

<sup>1</sup> Departamento de Física, Universidade Federal do Espírito Santo, Avenida Fernando Ferrari 514, Goiabeiras, 29075-910, Vitória, ES, Brazil

<sup>2</sup> Centro Brasileiro de Pesquisas Físicas, Rua Dr Xavier Sigaud 150, Urca, 22290-180, Rio de Janeiro, Brazil

<sup>3</sup> Instituto de Física de São Carlos, Universidade de São Paulo, PO Box 369, 13560-970, São Carlos, SP, Brazil

E-mail: [jair@npd.ufes.br](mailto:jair@npd.ufes.br)

Received 25 October 2007, in final form 7 January 2008

Published 14 February 2008

Online at [stacks.iop.org/JPhysCM/20/095214](http://stacks.iop.org/JPhysCM/20/095214)

## Abstract

Polycrystalline  $\text{La}_{0.86}\text{Sr}_{0.14}\text{Mn}_{1-x}\text{Cu}_x\text{O}_{3+\delta}$  ( $x = 0, 0.05, 0.10, 0.15, 0.20$ ) manganites were investigated by means of magnetic measurements and zero-field  $^{139}\text{La}$  and  $^{55}\text{Mn}$  nuclear magnetic resonance (NMR) spectroscopy. Magnetization versus temperature measurements revealed a paramagnetic to ferromagnetic transition in most samples, with lower Curie temperatures and broader transitions for samples with higher Cu contents. The details of the magnetization measurements suggested a phase-separated scenario, with ferromagnetic clusters embedded in an antiferromagnetic matrix, especially for the samples with large Cu contents ( $x = 0.15$  and  $0.20$ ). Zero-field  $^{139}\text{La}$  NMR measurements confirmed this finding, since the spectral features remained almost unchanged for all Cu-doped samples, whereas the bulk magnetization was drastically reduced with increasing Cu content.  $^{55}\text{Mn}$  NMR spectra were again typical of ferromagnetic regions, with a broadening of the resonance line caused by the disorder introduced by the Cu doping. The results indicate a coexistence of different magnetic phases in the manganites studied, with the addition of Cu contributing to the weakening of the double-exchange interaction in most parts of the material.

(Some figures in this article are in colour only in the electronic version)

## 1. Introduction

The issue of phase separation in colossal magnetoresistive manganites (compounds  $(\text{R},\text{A})\text{MnO}_{3+\delta}$ , with R—rare earth; A—alkaline earth) has attracted great interest from the scientific community in recent years. At present it seems to be generally accepted that the establishment of an inhomogeneous ground state is a general feature for many manganites and also for other strongly correlated systems [1, 2], for a wide range of compositions and temperatures. The evidence supporting this scenario comes from several different experimental methods, including conventional measurements of magnetic

and transport property measurements as well as techniques of a more local character such as neutron diffraction and nuclear magnetic resonance (NMR), among others [2–7]. The existence of minority phases dispersed in an overall matrix with different electronic properties was first suggested for interpreting the characteristics of materials in a magnetically ordered state. At low temperatures, a heterogeneous magnetic scenario was frequently invoked to account for some puzzling properties of these systems, usually pointing to a spin-glass or cluster-glass state [2, 3]. Also, recent results showed that even above the magnetic ordering temperature there is compelling evidence for the occurrence of a clustered state, with the presence of short-range ordered ferromagnetic clusters leading

<sup>4</sup> Author to whom any correspondence should be addressed.

to unusual properties for materials expected to be in an overall paramagnetic state [5, 8–10].

Since the magnetic and electronic properties of manganites are essentially controlled by interactions between Mn ions intermediated by O ions, an interesting way to better understand the intrinsic properties of manganese perovskites is by substituting at the Mn site, usually with other transition metal elements. Cu substitution has been particularly investigated due to its importance in the study of closely related cuprate superconductors, and valuable information about structure, magnetic and transport properties has been obtained for Cu-substituted manganites [11–15]. The substitution of Mn by Cu is readily accomplished for Cu atomic contents of up to 60% [16, 17]. This substitution leads to a change in the relative fraction of different valence Mn ions, since the addition of  $\text{Cu}^{2+}$  ions requires an increase in the fraction of  $\text{Mn}^{4+}$  ions in order to preserve the charge neutrality [17].

The Cu for Mn substitution causes marked modifications in the physical properties of manganites. The most immediate effect is the disruption of the double exchange between Mn ions, due to the presence of extraneous Cu ions. The consequence is the weakening of the ferromagnetic character of the material, which is reflected in the decrease of the Curie temperature and eventually in the suppression of the ferromagnetic order [11]. Also the transport properties are changed, with formation of domains with enhanced electron mobility as compared to other regions [12]. From the structural point of view, the introduction of Cu ions in the crystalline lattice leads to a steady decrease in the lattice parameters, although no modification of the crystal symmetry has been observed [16–18]. Other reported effects associated with the Cu for Mn substitution are the increases in catalytic activity in hydrogen oxidation processes [19] and in the magnitude of colossal magnetoresistance [20, 21] and magnetocaloric effect [10, 22].

This work aims to investigate the effect of Cu substitution on the magnetic properties of  $\text{La}_{0.86}\text{Sr}_{0.14}(\text{Mn}, \text{Cu})\text{O}_{3+\delta}$  manganites, both from bulk magnetization measurements and zero-field NMR spectroscopy. Although, as mentioned above, many structural and magnetic aspects associated with the Cu substitution have already been fully discussed in previous works, this is, to the best of our knowledge, the first detailed report on combined  $^{139}\text{La}$  and  $^{55}\text{Mn}$  NMR measurements on Cu-substituted manganites. With this approach, complemented by the characterization of bulk magnetic properties, we achieve, by using  $^{139}\text{La}$  and  $^{55}\text{Mn}$  nuclei as probes, detailed information about the local magnetic aspects of the manganites studied here and compelling evidence for the phase separation scenario for these materials.

## 2. Experimental methods

Polycrystalline samples of  $\text{La}_{0.86}\text{Sr}_{0.14}\text{Mn}_{1-x}\text{Cu}_x\text{O}_{3+\delta}$  with  $x = 0, 0.05, 0.10, 0.15$  and  $0.20$  were synthesized by the usual solid-state reaction technique, starting from stoichiometric mixtures of  $\text{La}_2\text{O}_3$ ,  $\text{SrCO}_3$ ,  $\text{MnO}_2$  and  $\text{CuO}$  powders. The final sintering was performed in an oxygen atmosphere at  $1400^\circ\text{C}$  for 30 min and this was followed by a period of

24 h at  $1300^\circ\text{C}$ . Powder x-ray diffraction (XRD) showed the formation of a rhombohedral  $R\bar{3}M$  structure for all samples, with decreasing unit cell volume and a small increase of lattice distortion for samples with larger values of  $x$ . From the XRD patterns, the values of the oxygen non-stoichiometry parameter  $\delta$  were estimated to be in the range  $0.023$ – $0.030$  [18]. The positive values of  $\delta$  indicate the presence of cation vacancies in the structure of the analysed compounds, associated with the oxygen-rich atmosphere used in the syntheses [16]. Scanning electron microscopy images revealed homogeneous microstructure in all samples, besides a trend for smaller grains and larger porosity with increasing Cu content. Energy dispersive x-ray spectrometry (EDS) showed local atomic contents in accordance with the nominal values. Further details on synthesis and structural characterization of these samples are reported elsewhere [18]. The magnetization measurements were carried out using a vibrating sample magnetometer in the temperature range from  $4.2$  to  $300$  K with magnetic fields up to  $25$  kOe. Both zero-field-cooling (ZFC) and field-cooling (FC) cycles were recorded. Zero-field  $^{139}\text{La}$  and  $^{55}\text{Mn}$  NMR spectra were recorded point by point using an automated pulsed NMR spectrometer from the spin-echo intensities measured at varying frequencies, with no external applied magnetic field and at a fixed temperature ( $4.2$  or  $77$  K). Typically, the pulse lengths were  $1$ – $2$   $\mu\text{s}$  and the pulse spacing was around  $2$   $\mu\text{s}$  for  $^{55}\text{Mn}$  and  $25$   $\mu\text{s}$  for  $^{139}\text{La}$  NMR measurements.

## 3. Results and discussion

### 3.1. Magnetic measurements

Figure 1(a) shows the temperature dependence of the DC magnetic susceptibility, obtained from the FC magnetization measured at low fields ( $200$ – $400$  Oe). The curves for the samples with  $x \leq 0.15$  show a well defined paramagnetic (PM) to ferromagnetic (FM) transition on cooling. The sample with  $x = 0.20$  exhibits a distinct behaviour, showing a much slower increase of the magnetization with decreasing temperature and a reduced magnetic moment at low temperatures. A slight drop in the magnetization for the samples with  $x = 0.15$  and  $0.20$  can also be observed at temperatures below about  $45$  K, suggesting the possibility of antiferromagnetic (AFM) ordering (at least in some regions of the material) around this temperature. The trends of reduction in the Curie temperatures, broadening of the transitions and decrease in the magnitude of the magnetization at low temperatures for samples with increasing Cu contents are in general agreement with previous works on Cu-substituted manganites [11, 23, 24].

From the data presented in figure 1(a), the following temperature values were obtained: the onset temperature for magnetic ordering ( $T_C^{\text{on}}$ ), determined from the point of intersection with the temperature axis of a tangent line traced at the point of maximum inclination of the  $\chi_{\text{DC}} \times T$  curve; the peak temperature for magnetic ordering ( $T_C^{\text{pk}}$ ), determined from the peak in the  $d\chi_{\text{DC}}/dT \times T$  curve; and the Curie–Weiss temperature ( $T_{\text{CW}}$ ), obtained by applying the Curie–Weiss law to the high-temperature  $\chi_{\text{DC}} \times T$  data. All these values are given in table 1. The difference between  $T_C^{\text{on}}$  and  $T_C^{\text{pk}}$  reflects

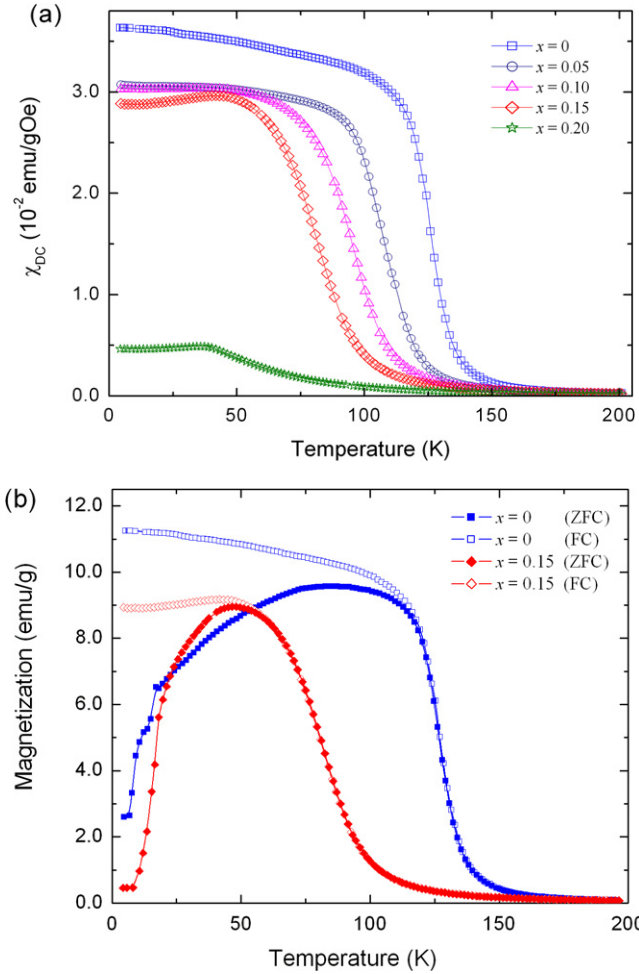


**Figure 1.** (a) Temperature dependence of the DC magnetic susceptibility for the samples with the indicated Cu contents. (b) ZFC and FC magnetization curves obtained for two typical samples with low applied magnetic fields (200 and 300 Oe for the samples with  $x = 0$  and 0.15, respectively).

the broadening of the magnetic transition and is therefore related to the degree of magnetic disorder or inhomogeneity in a given material. As can be seen in table 1, this difference is larger for all Cu-containing samples as compared to the undoped sample. Also, the values of  $T_C^{\text{on}} - T_C^{\text{pk}}$  are roughly constant (around 15 K) for the samples with  $x = 0.05\text{--}0.15$ , but the value corresponding to the sample with  $x = 0.20$  is still larger (37 K). On the other hand, the extent by which  $T_{\text{CW}}$  is greater than  $T_C^{\text{on}}$  is usually interpreted as an indication of the existence of short-range ferromagnetic correlations in the paramagnetic regime. Once more, the values of  $T_{\text{CW}} - T_C^{\text{on}}$  are roughly constant (15–19 K) for the samples with  $x = 0.05\text{--}0.15$ . This value is much higher than the ones found for both the undoped sample (4 K) and the sample with  $x = 0.20$  (1 K).

It is worth mentioning that the  $T_C$  values reported for the samples analysed in the present work (including the  $x = 0$  sample) are somewhat lower than the values expected based on the well-established phase diagrams for (La, Sr) manganites [25, 26]. This effect can be understood considering that the actual physical properties of a given

**Table 1.** Magnetic transition temperatures for samples with the indicated Cu contents (see the text for definitions).

| $x$  | $T_{\text{irr}}$ (K) | $T_C^{\text{pk}}$ (K) | $T_C^{\text{on}}$ (K) | $T_{\text{CW}}$ (K) |
|------|----------------------|-----------------------|-----------------------|---------------------|
| 0    | 120                  | 127                   | 135                   | 139                 |
| 0.05 | 95                   | 111                   | 126                   | 144                 |
| 0.10 | 77                   | 98                    | 113                   | 132                 |
| 0.15 | 57                   | 82                    | 99                    | 114                 |
| 0.20 | 38                   | 46                    | 83                    | 84                  |

manganite sample are greatly affected by the conditions of preparation, which influence the occurrence of oxygen non-stoichiometry, cation vacancies, local structural defects, etc [27–29]. All these effects can contribute to the low values of the Curie temperatures and broad magnetic transitions, especially considering that the compounds analysed here are in the region of the phase diagram of the (La, Sr) manganites where the  $T_C$  values present the steepest variation with the Sr atomic content [25]. Nevertheless, this does not invalidate the analysis of the effect of the Cu substitution, which is the main focus of the present work, since all samples were prepared under the same operational conditions and, as shown before, a systematic effect caused by the Cu substitution was readily observed in the magnetic properties of the analysed samples.

All these samples, including the undoped one ( $x = 0$ ), show thermal hysteresis when ZFC and FC cycles are compared, as shown in figure 1(b) for two typical samples. Such behaviour—which could be masked by the use of higher magnetic fields—is known to occur in various different classes of magnetic materials, including ferromagnetic materials with large magnetocrystalline anisotropy, nanoparticles, spin glasses, cluster glasses, etc [3, 20, 30–33]. In the case of the manganites analysed here, the thermomagnetic irreversibility is more likely to be related to the formation of a clustered state at low temperatures, as also suggested by the other experimental evidence discussed below. The values of the irreversibility temperature ( $T_{\text{irr}}$ ), defined as the temperature below which the FC and ZFC magnetization curves start to separate, are also given in table 1 for each sample.

Figure 2 shows the field dependent magnetization curves at fixed temperature (4.2 K) for the  $\text{La}_{0.86}\text{Sr}_{0.14}\text{Mn}_{1-x}\text{Cu}_x\text{O}_{3+\delta}$  samples. The results clearly indicate that samples with  $x \leq 0.15$  are typical ferromagnets, for which the magnetization shows a sharp increase followed by an approach to saturation (which is not reached for the range of magnetic fields employed here). The behaviour observed for the  $x = 0.20$  sample is somewhat different, with a much slower increase of the magnetization with the applied magnetic field (in agreement with the reduced magnetic susceptibility shown in figure 1(a)). The magnetization curve of this sample suggests a small FM component also in this composition, in agreement with the positive  $T_{\text{CW}}$  value obtained for this sample (see table 1).

The values of the saturation magnetization  $M_S$ , obtained by extrapolating the linear part of the  $M \times H^{-1}$  curves to  $H^{-1} = 0$ , are shown in table 2. For all samples  $M_S$  is much smaller than  $M_S^{\text{max}}$ , the expected value calculated considering spin-only contributions from  $\text{Mn}^{3+}$ ,  $\text{Mn}^{4+}$ , and

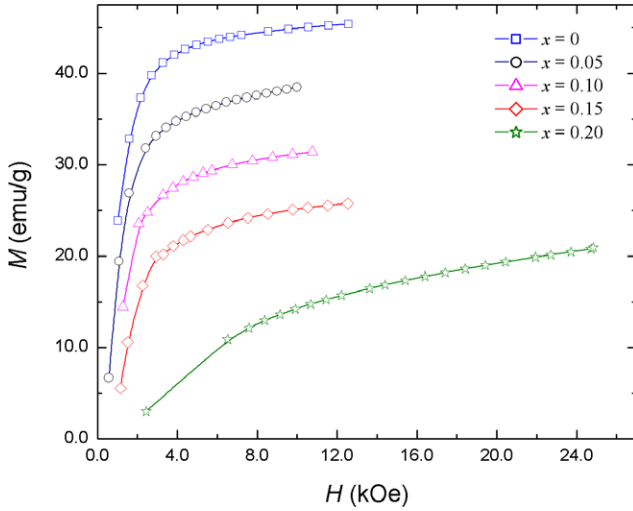


**Figure 2.** Field dependence of the magnetization recorded at 4.2 K for the samples with the indicated Cu contents.

**Table 2.** Magnetic data for samples with the indicated Cu contents (see the text for definitions).

| $x$  | $M_S$<br>( $\mu_B/\text{Mn}$<br>site) | $M_S^{\text{max}}$<br>( $\mu_B/\text{Mn}$<br>site) | $M_S/M_S^{\text{max}}$<br>(%) | $\mu_{\text{eff}}$<br>( $\mu_B/\text{Mn}$<br>site) | $\mu_{\text{calc}}$<br>( $\mu_B/\text{Mn}$<br>site) |
|------|---------------------------------------|--|-------------------------------|--|---|
| 0    | 1.99                                  | 3.80   | ~52                           | 5.7  | 4.69  |
| 0.05 | 1.79                                  | 3.60   | ~50                           | 4.7  | 4.48  |
| 0.10 | 1.43                                  | 3.40   | ~42                           | 5.4  | 4.28  |
| 0.15 | 1.20                                  | 3.20   | ~38                           | 6.2  | 4.07  |
| 0.20 | 1.19                                  | 3.01   | ~40                           | 6.6  | 3.87  |

$\text{Cu}^{2+}$  ions [17, 34] and also taking into account the small contribution due to the oxygen non-stoichiometry. This discrepancy also suggests the presence of FM clusters embedded in a non-ferromagnetic matrix as responsible for the magnetization values attained in high magnetic field. It is interesting to note that this seems to be true even for the undoped ( $x = 0$ ) and the low-doped ( $x \leq 0.10$ ) samples, indicating that the establishing of an overall inhomogeneous state is a general feature found even in the absence of Cu substitution. This effect is obviously enhanced by the disorder caused by the presence of Cu atoms, as can be seen by the reduced  $M_S/M_S^{\text{max}}$  ratios of the samples with  $x = 0.15$  and 0.20.

The formation of FM clusters is also corroborated by the analysis of the values of the effective magnetic moment ( $\mu_{\text{eff}}$ ) in the paramagnetic state, which are also given in table 2. These values were determined from the slope of the high-temperature  $\chi_{\text{DC}}^{-1} \times T$  curves, shown in figure 3 for the samples with  $x = 0$  and 0.15. The calculated values ( $\mu_{\text{calc}}$ ) considering the spin-only contributions discussed above are also included in table 2. It can be clearly seen that the  $\mu_{\text{eff}}$  values are systematically higher than  $\mu_{\text{calc}}$ , and the difference is greater for the samples with  $x = 0.15$  and 0.20. This strongly suggests the occurrence of FM clusters in the paramagnetic regime for all samples [26], and it is clear that this effect is accentuated by the Cu for Mn substitution.

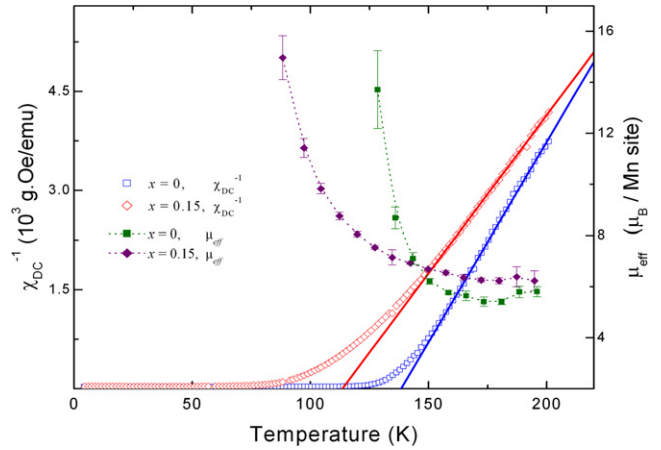


**Figure 3.** Temperature dependence of the inverse of the DC magnetic susceptibility for the samples with the indicated Cu contents, with the corresponding linear fittings. Also shown are the plots of the effective magnetic moments in the paramagnetic state (dotted lines are guides for the eyes).

It is worth commenting that the behaviour of the  $\chi_{\text{DC}}^{-1} \times T$  curves above  $T_C$  is not perfectly linear, especially in the case of the samples with higher Cu contents. This can be seen also in figure 3, where one includes the plots of the values of  $\mu_{\text{eff}}$  obtained by fitting the  $\chi_{\text{DC}}^{-1} \times T$  curves in small temperature intervals (around 7 K). A progressive drop of  $\mu_{\text{eff}}$  can be observed above  $T_C$ , but the slow asymptotic decrease suggests that the highest temperature employed in these measurements is not enough for the attainment of a truly linear behaviour. This is in agreement with previous works on manganites presenting a clustered state as a consequence of chemical and structural disorder induced by cation substitution [9].

### 3.2. $^{139}\text{La}$ NMR spectra

Zero-field  $^{139}\text{La}$  NMR signals have been detected in the 18–25 MHz range at 4.2 K for all samples; the spectra are shown in figure 4(a) for the samples with different Cu contents. The main peaks in these spectra are found near 22 MHz (corresponding to a hyperfine field around 3.7 T), and their linewidths are about 1 MHz. The most remarkable feature of these spectra is the observation of resonance lines with similar shapes and at the same frequency range for all samples, in spite of their very different bulk magnetic behaviour discussed before. The central line at about 22 MHz observed for all samples is associated with the response of  $^{139}\text{La}$  nuclei in a FM environment. As the  $\text{La}^{3+}$  ions are non-magnetic, the  $^{139}\text{La}$  NMR frequency reflects the transferred hyperfine field  $B_{\text{hf}}$ , from neighbouring Mn ions (with the most relevant contribution coming from the eight nearest neighbours). In a perfect AFM environment the resultant  $B_{\text{hf}}$  is close to zero, and zero-field  $^{139}\text{La}$  NMR lines associated with an AFM phase are not usually observed (or, if so, they would be observed at much lower frequencies) [6, 35, 36]. Therefore, one can associate all NMR spectra shown in figure 4(a) with a FM phase. In contrast to the magnetization results, the spectra features do not show significant variations with the increase

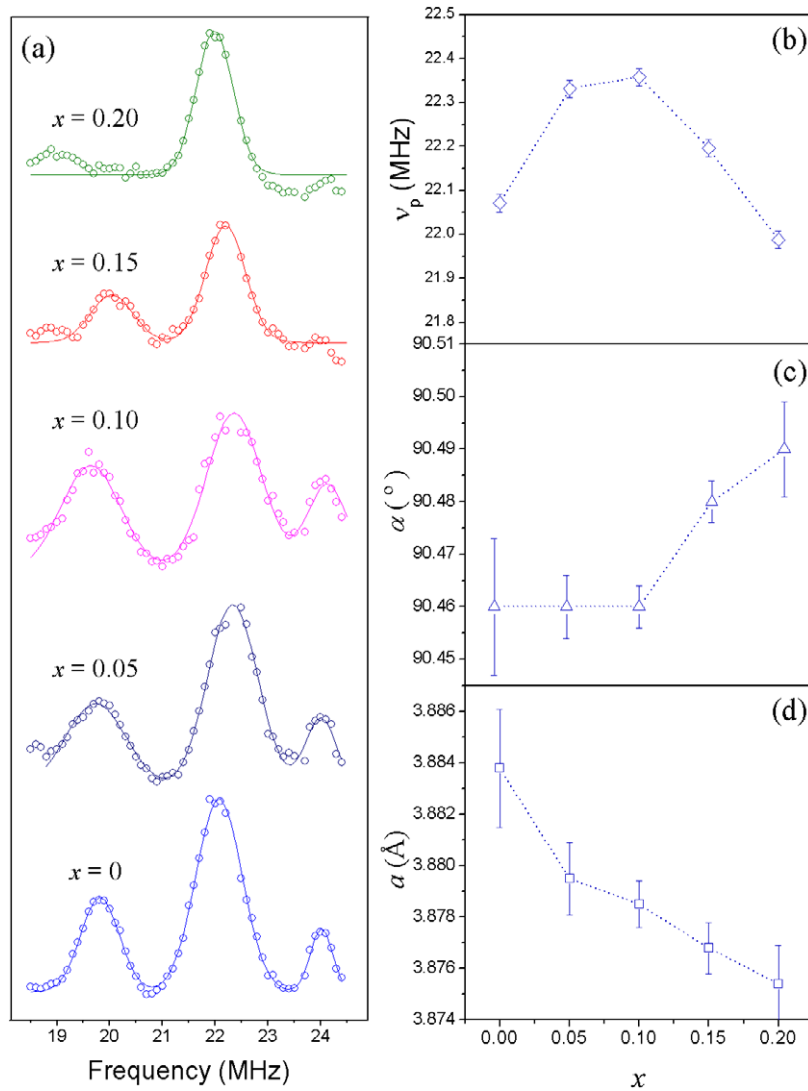


**Figure 4.** Zero-field  $^{139}\text{La}$  NMR spectra of the manganite samples recorded at 4.2 K (a) and Cu content dependence of the (b) central peak frequency, (c) rhombohedral angle of the unit cell and (d) lattice parameter of the rhombohedral unit cell. The solid lines in (a) indicate Gaussian fittings and the dotted lines in (b)–(d) are guides to the eyes. Data for structural parameters are taken from [18].

in Cu content, indicating similar FM regions in all samples. This finding is most striking for the  $x = 0.20$  sample, which presents a magnetic behaviour very different from those of the other samples, as can be seen in figures 1(a) and 2.

As discussed before, the magnetic results for this sample suggest the establishment of FM clusters dispersed in an AFM matrix. In this scenario, the NMR signals detected are solely due to the FM minority phase, which explains the similarity in the spectral features observed in the  $^{139}\text{La}$  NMR spectrum of this sample compared to the others. These FM clusters represent a minor contribution to the bulk magnetization data previously discussed. However, as the NMR signals due to non-ferromagnetic phases are not detectable in zero-field  $^{139}\text{La}$  NMR, the spectra shown in figure 4 are only due to the minor FM contributions, thus evidencing the inhomogeneous character of the Cu-substituted manganites.

A more detailed analysis of the value of the peak frequency reveals a small and smooth displacement of the central peak as a function of  $x$  (figure 4(b)). This feature

can be associated with slight structural changes caused by the Cu for Mn substitution [18], as shown in figures 4(c) and (d). As mentioned above, the  $^{139}\text{La}$  NMR frequency in zero-field measurements is dictated by the magnitude of the transferred hyperfine field, from neighbouring Mn ions, which depends on the overlap of the Mn  $t_{2g}$  orbitals with the on-site La  $s$  orbitals, mediated by p oxygen orbitals [6]. Assuming an isotropic hyperfine coupling and disregarding the small deviation from cubic symmetry [36], this magnetic field can be simply written as  $B_{\text{hf}} = A\langle S \rangle$ , where  $A$  is a constant (related to the constant of hyperfine coupling between the electronic magnetic moment of Mn ions and the  $^{139}\text{La}$  nucleus) and  $\langle S \rangle$  represents the mean electronic spin value of the eight Mn ions closest to a given  $^{139}\text{La}$  nucleus [6, 36]. The decrease of the Mn–O bond length with increasing Cu content, reflected in the shortening of the rhombohedral lattice parameter  $a$  (figure 4(d)), leads to an increase of the hyperfine coupling, implying higher values of  $B_{\text{hf}}$  and thus higher peak frequencies. However, for the samples with  $x = 0.15$  and  $0.20$ , the observed increase in

the distortion of the rhombohedral structure (figure 4(c)) can cause a decrease in the value of  $A$ , lowering  $B_{\text{hf}}$  in these two samples. Similar trends for changes of zero-field  $^{139}\text{La}$  NMR frequencies as a function of variations in the structural parameters have been reported for other manganites (without Cu doping) [6, 37].

Another interesting feature of the  $^{139}\text{La}$  NMR spectra shown in figure 4(a) is the observation of satellite lines on both sides of the central maximum. The exact nature of these extra peaks is not clear, and the low signal-to-noise ratio of the spectra makes it difficult to extract further information about them. It is worth noting, however, that  $^{139}\text{La}$  is a quadrupolar nucleus (spin  $7/2$ ), and therefore it is possible that the satellites are due to a coupling of the nuclear electric quadrupole moment of  $^{139}\text{La}$  with the electric field gradient (EFG) at the nuclear position. The EFG should be zero for an ideal perovskite structure, but the lack of cubic symmetry in the rhombohedral structure can clearly lead to a non-zero EFG at the  $^{139}\text{La}$  nuclei. If that is the case, one can estimate from the separation between the satellites and the central peak the magnitude of the quadrupolar frequency parameter ( $\nu_q$ ), which is around 2.5 MHz for all samples where the satellites were detected. This value is of the same order of magnitude as the  $\nu_q$  values reported for other similar manganites [38–41].

However, the direct observation of the quadrupolar split spectrum is rarely reported for manganites; usually only at high temperatures can the satellites be explicitly detected, since for the magnetically ordered states the existence of distributions of magnetic shifts swamps the typical features of a quadrupolar pattern [38, 42]. The fact that the signals observed in this work are due only to spatially restricted FM regions (and not to the bulk of the samples) can be perhaps invoked as a possible reason for the reduced magnetic broadening of the resonance lines. In fact, the linewidths of the observed peaks are around 1 MHz in the present case, compared to typically 5–8 MHz linewidths in other manganites reported in the literature. This could justify the direct observation of the quadrupolar satellite lines. It is worth mentioning, however, that other explanations have been mentioned in the literature for the existence of resolved peaks in  $^{139}\text{La}$  NMR spectra of manganites (both in zero-field NMR and in measurements conducted under external field), such as the occurrence of inhomogeneous spin arrangements in FM domains [36] and the possibility of increased covalence for some La ions with the nearest neighbour Mn ions [43]. The elucidation of the origin of the satellite peaks in the present  $^{139}\text{La}$  NMR spectra is therefore an issue that demands further work, with methods specifically suited for the investigation of the effects of the quadrupolar interaction, such as measurements at different applied magnetic fields or the search for quadrupolar oscillations in time-domain signals.

### 3.3. $^{55}\text{Mn}$ NMR spectra

$^{55}\text{Mn}$  NMR spectra of Cu-doped samples have been observed in the 300–450 MHz range. The comparison of the spectra shown in figure 5(a) for samples with compositions  $\text{La}_{0.86}\text{Sr}_{0.14}\text{MnO}_{3+\delta}$  and  $\text{La}_{0.86}\text{Sr}_{0.14}\text{Mn}_{0.90}\text{Cu}_{0.10}\text{O}_{3+\delta}$  indicate

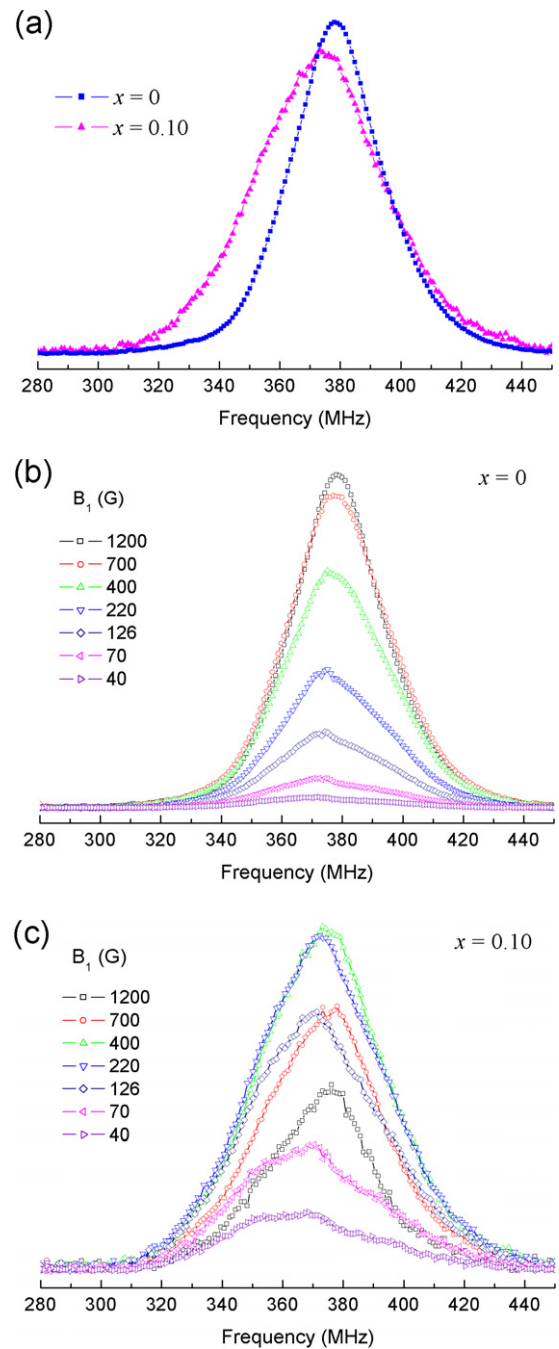


**Figure 5.** (a) Zero-field  $^{55}\text{Mn}$  NMR spectra recorded at 77 K for samples with the indicated Cu contents. Spectra acquired with different RF strengths ( $B_1$  fields) are shown for the samples with  $x = 0$  (b) and  $x = 0.10$  (c). The spectra shown in (a) correspond to the  $B_1$  values that give the maximum signal for each sample.

a slight reduction in the average hyperfine field along with a broadening of the resonance line, caused by the disorder introduced by the Cu doping. The analysis of the change in the  $^{55}\text{Mn}$  NMR spectra with change in the RF strength (measured by the value of the amplitude of the RF magnetic field,  $B_1$ ) is shown in figures 5(b) and (c) for both samples. All lines detected from zero-field  $^{55}\text{Mn}$  NMR measurements are again typical of FM regions, since NMR lines coming from AFM regions would have no RF enhancement due to the coupling of

the nuclear magnetic moment to the electronic magnetization, and therefore would require an RF power much higher than the resonance lines associated with FM environments [35].

Unlike the  $^{139}\text{La}$  case, the hyperfine field at the  $^{55}\text{Mn}$  nuclei is mostly due to an intra-ionic contribution, caused by the non-zero electronic magnetic moment of the Mn ions. In zero-field NMR, the values of the resonance frequencies are thus dictated by the on-site spin value of each ion, and therefore  $^{55}\text{Mn}$  NMR probes the electronic state of the different Mn ions present in the material. On the basis of previous results in the literature, the typical values of resonance frequencies for zero-field  $^{55}\text{Mn}$  NMR in magnetically ordered manganites for localized  $\text{Mn}^{4+}$  ions (with electronic spin = 3/2) lie around 320 MHz and the lines are reasonably sharp and well defined. For localized  $\text{Mn}^{3+}$  ions, on the other hand, which have electronic spin = 2 and a strong anisotropic contribution due to the extra electron in the  $e_g$  orbital, the lines are excessively broad, extending typically from 400 MHz upward. A single ‘motionally averaged’ line at about 380 MHz is usually observed for metallic regions, where the fast electron (or hole) motion leads to an average hyperfine field intermediate between the two values given above [6, 35, 44–47].

On the basis of these assignments, it is clear that the resonance line detected for the sample with  $x = 0$  in figure 5(a) is due to regions with fast hopping of electrons/holes, associated with a FM metallic phase. The spectrum observed for the sample with  $x = 0.10$  is also dominated by a resonance centred around 374 MHz, but in this case there is a clear increase in the intensity in the range 320–360 MHz, giving rise to a broad shoulder in this spectrum. This shoulder is likely to be associated with  $\text{Mn}^{4+}$  ions, whose concentration increases with Cu doping, as discussed above.

The analysis of the spectra acquired with different  $B_1$  values show different behaviours for the two samples. In the case of the sample with  $x = 0$ , the signal intensity increases progressively with the increase in  $B_1$ , which is accompanied by a narrowing of the resonance. For the sample with  $x = 0.10$ , on the other hand, the maximum signal is recorded for a  $B_1$  value of 400 G. Again a slight narrowing is observed with increasing  $B_1$ , along with a shift of the peak to high frequency. These changes in the spectral characteristics with the change in the RF field are indicative of the presence of ferromagnetic regions with different magnetocrystalline anisotropy field ( $B_A$ ). For ferromagnetic materials, the regions with low  $B_A$  values are associated with large RF enhancement factors due to the hyperfine coupling and thus give rise to strong signals at low values of the  $B_1$  field [48]. It is worth noting that in domain walls this effect is much more pronounced, with enhancement factors higher by several orders of magnitude than within the domains, due to the high susceptibility of reversible displacements of the walls. Therefore, signals associated with domain walls are usually recorded in  $B_1$  fields much smaller than the ones corresponding to domain cores. On the basis of these facts and considering that all spectra shown in figure 5 have been recorded with reasonably high  $B_1$  values and all in the same range, one can conclude that these spectra correspond to ferromagnetic domains and not to domain walls. This reasoning is in agreement with the previously discussed

scenario of small FM islands surrounded by an AFM matrix, which excludes the formation of a domain structure in the material.

The results shown in figures 5(b) and (c) thus reveal that the contributions associated with  $\text{Mn}^{4+}$  ions, occurring in the range 320–360 MHz, correspond to regions with lower  $B_A$ , being therefore easily detected for low  $B_1$  values especially in the case of the Cu-doped sample. On the other hand, the dominant signal at 375–380 MHz, which is due to regions with fast moving electrons/holes, corresponds to regions of higher anisotropy fields. The coexistence of ferromagnetic regions with distinct dynamic behaviour and different magnetocrystalline anisotropy has been reported by Savosta *et al* for a number of other manganites [46, 47]. In such cases, the signal at lower frequency ( $\sim 330$  Hz) was attributed to quasi-localized  $\text{Mn}^{4+}$  ions in regions of ferromagnetic insulating character and weakened double-exchange interaction. A similar situation is likely to occur in the manganites studied here, where the addition of  $\text{Cu}^{2+}$  ions leads to an increase in the fraction of  $\text{Mn}^{4+}$  ions and to a decline of the double-exchange interaction, contributing to the establishing of a phase-separated scenario in the materials.

Therefore, the set of magnetization,  $^{139}\text{La}$ , and  $^{55}\text{Mn}$  NMR data all point to a mixed magnetic phase in these compounds. As it has been suggested that the presence of  $\text{Cu}^{2+}$  cations in the Mn sublattice induces the AFM superexchange interaction and suppresses the FM double-exchange interaction in the manganites [11], the results above can be consistently interpreted in a scenario involving a mixed FM/AFM state, with an increasing contribution from the AFM phase for samples with higher Cu contents.

## 4. Conclusion

Polycrystalline samples of  $\text{La}_{0.86}\text{Sr}_{0.14}\text{Mn}_{1-x}\text{Cu}_x\text{O}_{3+\delta}$  with  $x = 0, 0.05, 0.10, 0.15,$  and  $0.20$  were synthesized and analysed by means of magnetic and NMR measurements. The magnetic properties were found to be quite sensitive to the Cu doping, which led to a lowering of the Curie temperature, broadening of the ordering transition, and reduction of the saturation magnetization. Zero-field  $^{139}\text{La}$  and  $^{55}\text{Mn}$  NMR results gave evidence of the existence of ferromagnetic clusters in all samples, which suggests an interpretation of the magnetic structure of the manganites studied in terms of a mixed magnetic phase state.

## Acknowledgments

The partial support from Brazilian agencies CNPq, CAPES, FINEP, and FAPESP is gratefully acknowledged. The authors are also grateful to Professor P Panissod (Université Louis Pasteur, Strasbourg) for helping with the  $^{55}\text{Mn}$  NMR measurements, to Dr M G das Virgens (Federal Fluminense University) for helping with the magnetic measurements and to Professor R F Jardim (University of São Paulo) for fruitful discussions and suggestions.

## References

- [1] Moreo A, Yunoki S and Dagotto E 1999 *Science* **283** 2034
- [2] Dagotto E 2003 *Nanoscale Phase Separation and Colossal Magnetoresistance. The Physics of Manganites and Related Compounds* (Berlin: Springer)
- [3] Freitas R S, Ghivelder L, Damay F, Dias F and Cohen L F 2001 *Phys. Rev. B* **64** 144404
- [4] Lynn J W, Erwin R W, Borchers J A, Huang Q, Santoro A, Peng J-L and Li Z Y 1996 *Phys. Rev. Lett.* **76** 4046
- [5] Matveev V V, Ylinen E, Zakhvalinskii V S and Laiho R 2007 *J. Phys.: Condens. Matter* **19** 226209
- [6] Papavassiliou G, Fardis M, Belesi M, Pissas M, Panagiotopoulos I, Kallias G, Niarchos D, Dimitropoulos C and Dolinsek J 1999 *Phys. Rev. B* **59** 6390
- [7] Martynov O, Yudanov V, Lee R, Volkov N and Sablina K 2007 *Phys. Status Solidi (RRL)* **1** R22
- [8] De Teresa J M, Ibarra M R, Algarabel P A, Ritter C, Marquina C, Blasco J, García J, del Moral A and Arnold Z 1997 *Nature* **386** 256
- [9] Souza J A and Jardim R F 2005 *Phys. Rev. B* **71** 054404
- [10] Zhao B C, Sun Y P, Zhu X B and Song W H 2007 *J. Appl. Phys.* **101** 053920
- [11] Pi L, Zheng L and Zhang Y 2000 *Phys. Rev. B* **61** 8917
- [12] Pi L, Xu X and Zhang Y 2000 *Phys. Rev. B* **62** 5667
- [13] Zheng L, Xu X, Pi L and Zhang Y 2000 *Phys. Rev. B* **62** 1193
- [14] Reis M S, Freitas J C C, Orlando M T D, Gomes A M, Lima A L, Oliveira I S, Guimarães A P and Takeuchi A Y 2002 *J. Magn. Magn. Mater.* **242–245** 668
- [15] Popovic Z V, Cantarero A, Thijssen W H A, Paunovic N, Dohcevic-Mitrovic Z and Sapiña F 2005 *J. Phys.: Condens. Matter* **17** 351
- [16] Porta P, De Rossi S, Faticanti M, Minelli G, Pettiti I, Lisi L and Turco M 1999 *J. Solid State Chem.* **146** 291
- [17] Belous A G, V'yunov O I, Yanchevskii O Z, Tovstolytkin A I and Golub V O 2006 *Inorg. Mater.* **42** 286
- [18] Victor R A, Orlando M T D and Freitas J C C 2007 *Quim. Nova* **30** 1517
- [19] Buciuman F-C, Patcas F, Menezes J-C, Barbier J, Hahn T and Lintz H-G 2002 *Appl. Catal. B* **35** 175
- [20] Yuan S L, Yang Y P, Xia Z C, Liu L, Zhang G H, Feng W, Tang J, Zhang L J and Liu S 2002 *Phys. Rev. B* **66** 172402
- [21] Yuan S L, Zhang L J, Xia Z C, Zhao L F, Liu L, Chen W, Zhang G H, Feng W, Tang J, Cao H, Zhong Q H, Niu L Y and Liu S 2003 *Phys. Rev. B* **68** 172408
- [22] Phan M-H, Peng H-X, Yu S-C, Tho N D and Chau N 2005 *J. Magn. Magn. Mater.* **285** 199
- [23] Yuan S L, Li Z Y, Zhang G Q, Tu F, Zeng X Y, Yang Y P and Tang C Q 2001 *Solid State Commun.* **117** 661
- [24] Haupt L, von Helmolt R, Sondermann U, Bärner K, Tang Y, Giessinger E R, Ladizinsky E and Braunstein R 1992 *Phys. Lett. A* **165** 473
- [25] Urushibara A, Moritomo Y, Arima T, Asamitsu A, Kido G and Tokura Y 1995 *Phys. Rev. B* **51** 14103
- [26] Paraskevopoulos M, Mayr F, Hemberger J, Loidl A, Heichele R, Maurer D, Müller V, Mukhin A A and Balbashov A M 2000 *J. Phys.: Condens. Matter* **12** 3993
- [27] Mitchell J F, Argyriou D N, Potter C D, Hinks D G, Jorgensen J D and Bader S D 1996 *Phys. Rev. B* **54** 6172
- [28] Abdelmoula N, Guidara K, Cheikh-Rouhou A, Dhahri E and Joubert J C 2000 *J. Solid State Chem.* **151** 139
- [29] Malavasi L, Ritter C, Mozzati M C, Tealdi C, Islam M S, Azzoni C B and Flor G 2005 *J. Solid State Chem.* **178** 2042
- [30] Chaudhary S, Roy S B and Chaddah P 2001 *J. Alloys Compounds* **326** 112
- [31] Joy P A, Kumar P S A and Date S K 1998 *J. Phys.: Condens. Matter* **10** 11049
- [32] Xue Y Y, Lorenz B, Cao D H and Chu C W 2003 *Phys. Rev. B* **67** 184507
- [33] Respaud M, Broto J M, Rakoto H, Fert A R, Thomas L, Barbara B, Verelst M, Snoeck E, Lecante P, Mosset A, Osuna J, Ely T O, Amiens C and Chaudret B 1998 *Phys. Rev. B* **57** 2925
- [34] Vertruyen B, Rulmont A, Cloots R, Ausloos M, Fagnard J-F, Dorbolo S and Vanderbemden Ph 2004 *J. Magn. Magn. Mater.* **268** 364
- [35] Allodi G, De Renzi R, Licci F and Pieper M W 1998 *Phys. Rev. Lett.* **81** 4736
- [36] Allodi G, De Renzi R and Guidi G 1998 *Phys. Rev. B* **57** 1024
- [37] Dho J, Kim I, Lee S, Kim K H, Lee H J, Jung J H and Noh T W 1999 *Phys. Rev. B* **59** 492
- [38] Sakaie K E, Slichter C P, Lin P, Jaime M and Salamon M B 1999 *Phys. Rev. B* **59** 9382
- [39] Kumagai K, Iwai A, Tomioka Y, Kuwahara H, Tokura Y and Yakubovskii A 1999 *Phys. Rev. B* **59** 97
- [40] Furukawa Y, Okamura I, Kumagai K, Goto T, Fukase T, Taguchi Y and Tokura Y 1999 *Phys. Rev. B* **59** 10550
- [41] Allodi G, Guidi M C, De Renzi R, Caneiro A and Pinsard L 2001 *Phys. Rev. Lett.* **87** 127206
- [42] Bastow T J 1994 *Solid State Nucl. Magn. Reson.* **3** 17
- [43] Yoshinari Y, Hammel P C, Thompson J D and Cheong S-W 1999 *Phys. Rev. B* **60** 9275
- [44] Matsumoto G 1970 *J. Phys. Soc. Japan* **29** 615
- [45] Anane A, Dupas C, Le Dang K, Renard J P, Veillet P, de Leon Guevara A M, Millot F, Pinsard L and Revcolevschi A 1995 *J. Phys.: Condens. Matter* **7** 7015
- [46] Savosta M M, Doroshev V D, Kamenev V I, Borodin V A, Tarasenko T N, Mazur A S and Marysko M 2003 *J. Exp. Theor. Phys.* **97** 573
- [47] Savosta M M, Kamenev V I, Borodin V A, Novák P, Marysko M, Hejtmánek J, Dörr K and Sahana M 2003 *Phys. Rev. B* **67** 094403
- [48] Guimarães A P 1998 *Magnetism and Magnetic Resonance in Solids* (New York: Wiley)